DESY 95-228
November 1995

DESY 95-228
ISSN 0418-9833

DEEP–INELASTIC ELECTRON–PROTON DIFFRACTION [1]

John B. Dainton

Oliver Lodge Laboratory,
Department of Physics,
The University of Liverpool[2],
P O Box 147, Liverpool L69 3BX, UK.[3]

for the H1 Collaboration at HERA

(June 1995)

Abstract

Recent measurements by the H1 collaboration at HERA of the cross section for deep–inelastic electron–proton scattering in which the proton interacts with minimal energy transfer and limited 4–momentum transfer squared are presented in the form of the contribution $F_2^{D(3)}$to the proton structure function F_2. By parametrising the cross section phenomenologically in terms of a leading effective Regge pole exchange and comparing the result with a similar parametrisation of hadronic pp physics, the proton interaction is demonstrated to be dominantly of a diffractive nature. The quantitative interpretation of the parametrisation in terms of the properties of an effective leading Regge pole exchange, the pomeron ($I\!P$), shows that there is no evidence for a "harder" BFKL–motivated $I\!P$ in such deep–inelastic proton diffraction. The total contribution of proton diffraction to deep–inelastic electron–proton scattering is measured to be $\sim 10\%$ and to be rather insensitive to Bjorken–x and Q^2. A first measurement of the partonic structure of diffractive exchange is presented. It is shown to be readily interpreted in terms of the exchange of gluons, and to suggest that the bulk of diffractive momentum transfer is carried by a leading gluon.

[1]Based on results from the H1 experiment at HERA presented at the International Workshop on Deep–Inelastic Scattering and Related Topics, Paris, France, April 1995, and at the VI Blois Workshop "Frontiers in Strong Interactions", Château de Blois, France, June 1995; available from http://dice2.desy.de/

[2]Supported by the UK Particle Physics and Astronomy Research Council and the University of Liverpool

[3]Present address: DESY(FH1T), 22603 Hamburg, Notkestrasse 85, Germany; e–mail: dainton@dice2.desy.de

1 Introduction

"Hadronic diffraction" originates from the observed dependence on scattering angle, or 4–momentum transfer squared t, of the cross section for hadron–hadron elastic scattering, for example $pp \to pp$. At high energy the dependence is very reminiscent of the diffraction patterns of optical physics. Over decades a phenomenology of "diffractive hadronic interactions" has grown up along side the accumulation of a wealth of experimental data. These data now also include measurements of the cross sections for inelastic diffractive interactions, for example $pp \to pX$. They are identified by t and centre of mass energy ($\sqrt{s}$) dependences which closely resemble those of elastic interactions.

The phenomenology is built on the analytic properties of hadronic scattering amplitudes as functions of kinematic variables such as s, t and angular momentum, and it succeeds in some cases in correlating many features of high energy hadron–hadron interactions in terms of relatively few parameters. However since the advent of QCD as the theory of hadronic physics, it has been clear that ultimately there must be an understanding of this phenomenology in terms of QCD. With the advent of the ep collider HERA, for the first time it has become possible to probe the regions of proton structure involved in the interactions which form the bulk of the proton interaction cross section at high energy. The first such measurements by the H1 experiment are reported here.

2 Deep ep Interactions and H1

The H1 experiment [1] at the HERA ep collider at DESY, Hamburg, is an hermetic detector which has operated taking data since the start–up of HERA, the first electron–proton (ep) collider, in summer 1992 (figure 1 shows graphics displays of two ep DIS interactions). It is optimised for efficient and accurate measurements of ep physics in an environment in which an 820 GeV proton (p) beam (always from the right) is incident head–on with a 27.6 GeV electron or positron (e) beam (always from the left). This asymmetry in colliding beam energies, which arises because of the usual limitation due to synchrotron radiation on e storage ring energy and which is also essential for precision measurement of scattered electrons at intermediate Q^2 ($\sim 1 < Q^2 \lesssim 100\,\mathrm{GeV}^2$), gives rise to greater instrumentation in the forward (proton beam) direction. Here a coordinate system is used with origin at the interaction point and z axis along the proton beam, or forward, direction. The pseudo–rapidity of a final state particle with polar angle θ in the laboratory is then $\eta = -\ln\tan\frac{\theta}{2}$. The very different r.f. structures of the proton and electron rings also pose the severe challenge to the experiment of e and p bunch crossings every 96 ns, a precursor for LHC experimentation. The solution is to implement "pipeline" technology in the data–acquisition stream.

Precision measurements of energy flow, charged particle production, and lepton (electron and muon) production is possible with H1 throughout a large range in laboratory pseudo–rapidity $-2.94 \leq \eta \leq 3.65$. This is achieved by means of a large asymmetric liquid argon calorimeter (LAr) with longitudinal segmentation appropriate for precision measurement of both electromagnetic ($\sigma_E/E \sim 12\%/\sqrt{E(\mathrm{GeV})} \oplus 1\%$, $\Delta E_{scale} \sim 2\%$) and hadronic ($\sigma_E/E \sim 50\%/\sqrt{E(\mathrm{GeV})} \oplus 2\%$, $\Delta E_{scale} \sim 5\%$) energy [2, 3]. ΔE_{scale} is the uncertainty in absolute value of the calorimeter energy scale. Inside the LAr is a comprehensive system of drift chambers and multi–wire proportional chambers for track measurement and triggering using charged particles originating from the z range of the event vertex (CTD, FTD). Outside the LAr is a large superconducting solenoid ($B = 1.18\,\mathrm{T}$) with an instrumented iron return yoke (CMD) plus in the forward direction a system of drift chambers and additional toroidal magnetic field

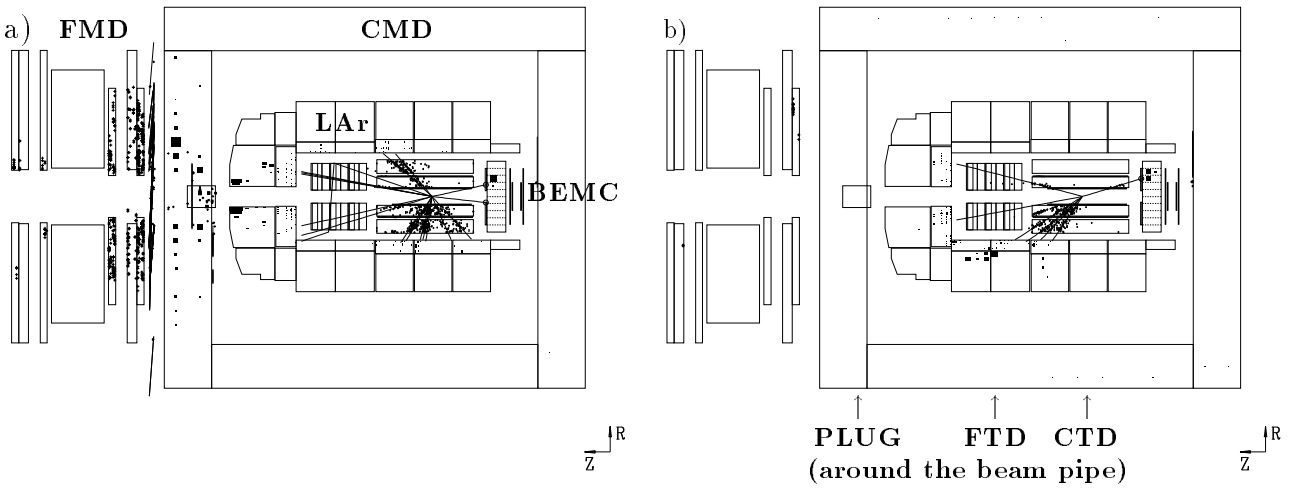

Figure 1: Two ep deep–inelastic scattering events measured in the H1 experiment at HERA. Electrons of energy 27.6 GeV are incident from the left and protons of energy 820 GeV from the right. Electrons are detected in the backward electromagnetic calorimeter (BEMC) to the right of the interaction point. Around the interaction point in order of increasing radius are the central and forward track detectors (CTD, FTD), the liquid argon calorimeter (LAr), the high field superconducting solenoid (not marked), and the muon detector (CMD). In a) hadronic fragments produced throughout the available phase space between the current direction and the forward (proton beam) direction. They are visible in the forward PLUG calorimeter and as secondaries in the forward muon detector (FMD). In b) is an ep deep–inelastic scattering event with a rapidity gap devoid of hadronic fragments adjacent to the proton beam direction in the forward region of LAr, PLUG and FMD.

(FMD) [4]. In the backward direction, scattered electrons (and positrons) are measured in the backward electromagnetic calorimeter (BEMC, electromagnetic energy resolution $\sigma_E/E \sim 10\%/\sqrt{E\,(\mathrm{GeV})}$, $\Delta E_{scale} \sim 1.5\%$) and in a multi–wire proportional chamber (BPC).

Two electromagnetic calorimeters (LUMI) situated downstream in the electron beam direction measure electrons and photons from the process $ep \to ep\gamma$ for the purpose of luminosity determination. They are also used to help quantify photoproduction background in deep–inelastic electron scattering.

In the forward direction $\eta > 3.65$, it is possible, using the "plug" calorimeter (PLUG), to "tag" the production of energy in the forward pseudo–rapidity range $3.54 < \eta < 5.08$ above a threshold of 1 GeV. Furthermore, using a novel technique [5] it is also possible to "tag" the production of hadrons in the forward pseudo–rapidity range $5.0 < \eta < 6.6$ by detecting and reconstructing track segments in the forward muon detector (FMD) due to charged particles produced in secondary interactions of these hadrons in the collimators, the beam pipe, and adjunct material.

In 1994 HERA delivered $6\,\mathrm{pb}^{-1}$ of integrated luminosity of which H1 used $3.9\,\mathrm{pb}^{-1}$ for physics analysis. These data consist of roughly 12×10^6 events on tape, which were recorded using triggers based on missing transverse energy in the LAr ($E_{T_{miss}} \gtrsim 6\,\mathrm{GeV}$), on track transverse momentum in CTD and FTD ($p_T \gtrsim 0.15\,\mathrm{GeV}$), on e energy in BEMC and BPC ($E_{BEMC} \gtrsim 4\,\mathrm{GeV}$ plus charged particle), and on e energy E_{LUMI} in LUMI ($0.3 < y\,(= 1 - E_{LUMI}/E_{beam}) < 0.7$). The integrated luminosity was measured with an accuracy of 1.5% (2%) for positron (electron) beam running. During positron beam running, the average $e(p)$ beam currents were 17(41) mA, and there were 168(170) $e(p)$ bunches in each ring of which 156 collided. The remaining bunches were not in collision at the interaction point and so could be used for determination of beam–gas and beam–wall/collimator backgrounds.

The configuration of the detectors which comprise H1 thus facilitates accurate reconstruction of the kinematic quantities specifying ep interactions of different nature. Furthermore, and in contrast with all its fixed target predecessors, for the first time subtle and powerful

measurements of the topological features of hadron production are possible by virtue of the excellent experimental coverage of the final state phase space.

3 Kinematics

The kinematics of deep–inelastic ep physics at HERA is conveniently classified into low Q^2 and high Q^2 processes. The former correspond to quasi–real photoproduction (γp) and the latter to electroproduction. Photoproduction is in the main taken to be events for which the quasi–real photon is defined by detection and measurement in LUMI of the incident electron or positron which scatters at very small angle. Except for purposes of comparison, none of the new physics presented here is concerned with diffraction in photoproduction.

High Q^2 deep–inelastic ep physics is of course best described in terms of the familiar "scaling variables" Bjorken–x x_{Bj} and Q^2 (M_p is the proton rest mass)

$$x_{Bj} = \frac{-q^2}{2P \cdot q} = \frac{Q^2}{Q^2 + W^2 - M_p^2} \approx x_{i/p} \qquad Q^2 = -q^2, \tag{1}$$

the former of which may be taken as the fraction of the 4–momentum of the incident proton $x_{i/p}$ carried by the "struck" parton, that is the parton coupling to the virtual photon (figure 2a). Here q and P are the 4–momenta of the virtual boson and the incident proton respectively. The scaling variable y is most easily specified as $Q^2/(sx_{Bj})$ where $\sqrt{s}$ is the ep centre of mass (CM) energy.

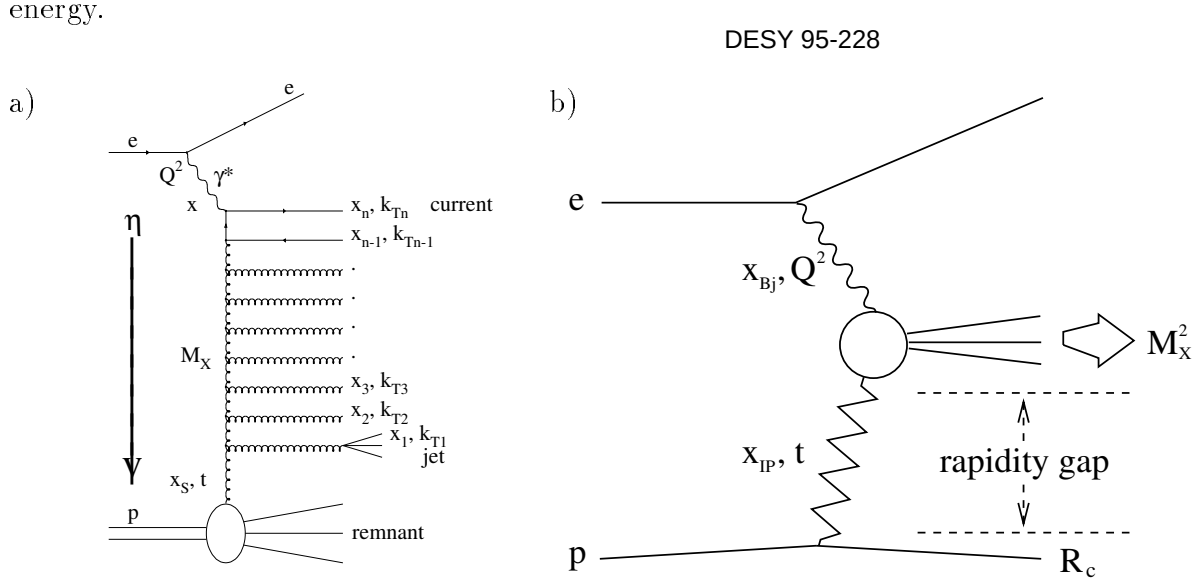

Figure 2: Schematic Feynman diagrams for a) ep DIS at low Bjorken–x illustrating how QCD can give rise to hadron production from partons produced between the "struck" or "current" quark at $x = x_n = x_{Bj}$ and the proton remnant; increasing pseudo–rapidity η from the current quark towards the remnant corresponds roughly to increasing the fractional momentum $x_{i/p} = x_i$ of the parton which forms the side of the "ladder"(usually a gluon at low Bjorken–x) as a fraction of the incident proton; the transverse momenta of the ith parton is k_{Ti}; and for b) a deep–inelastic ep interaction in which there is a forward diffractive "rapidity gap" devoid of hadronic energy; the high Q^2 virtual photon interacts with a colourless entity of space–like mass t whose momentum as a fraction of the target proton is $x_{I\!P}$; a (colourless) remnant of the proton R_c continues close to the incident direction of the target proton in the laboratory frame.

However at HERA the immense ep CM energy, and the access to the final state hadronic phase space in the form of the large coverage in pseudo–rapidity η afforded by the colliding beam laboratory frame, mean that this well known picture can be extended. Suppose that a proportion, M_X, of the total hadronic invariant mass W (W equals the $\gamma^* p$ CM energy) can

be defined in an interval of η adjacent to the direction of the current quark (figure 2). Then, the fraction of the 4–momentum of the incident proton carried by the system S, $x_{S/p}$, which together with the virtual photon constitutes X, can be related to an invariant quantity x_S by

$$x_S = \frac{q \cdot (P - P')}{q \cdot P} = \frac{Q^2 + M_X^2 - t}{Q^2 + W^2 - M_p^2} \approx \frac{Q^2 + M_X^2}{Q^2} \cdot x = x_{S/p}. \tag{2}$$

Also the fraction of the 4–momentum of S carried by the quark, $x_{q/S}$, coupling to the virtual photon can be related to an invariant quantity β by

$$\beta = \frac{-q^2}{2q \cdot (P - P')} = \frac{Q^2}{Q^2 + M_X^2 - t} \approx \frac{Q^2}{Q^2 + M_X^2} = x_{q/S}. \tag{3}$$

Here the 4–vector of S is specified by $P - P'$ and its space–like mass squared by $t = (P - P')^2$. Note as expected that

$$x = \beta \cdot x_S, \tag{4}$$

and that the compact interpretation of x, x_S and β as fractional momenta are only valid in the low "mass" limits $|\, t \,|$, $M_p^2 \ll Q^2, M_X^2$. In the cases normally considered, namely when S is a gluon from the proton [6] or S is a colourless momentum transfer coupling to the proton (the situation with which we are concerned here), t easily meets such a requirement. The simple multiplicative relationship in equation 4 between fractional momenta x, β and x_S is a specific example of the fact that moving in pseudo–rapidity η from the current towards the proton remnant corresponds to fractional momenta x increasing from x_{Bj} such that $\Delta \ln x = \Delta\eta$.

4 The Leading Rapidity Gap Phenomenon in DIS

Following the ZEUS experiment [7], DIS ep events were reported in 1993 [8, 9] by H1 in which a leading "rapidity gap" phenomenon was observed in the forward direction (see figure 1 for examples of DIS events with and without a forward rapidity gap). In a search for intervals of laboratory pseudo–rapidity which are devoid of hadronic energy ($E_{had} < 400\,\mathrm{MeV}$ at the finest "cell" level of LAr segmentation), a scatter plot (figure 3a) of the largest such interval $\Delta\eta$ against the pseudo–rapidity of the forward end of $\Delta\eta$ in the LAr demonstrates that the leading "rapidity gap" effect is empty intervals adjacent to the most forward acceptance ($\eta = 3.65$). Such events were anticipated [10, 11] as the manifestation of diffractive $\gamma^* p$ physics.

Much can be inferred from the simple observation of such "rapidity gaps". Any such phenomenon in which the distribution of gap size is not exponentially suppressed in the overall CM ($\gamma^* p$) frame has been taken by Feynman and Bjorken [11, 12] as the definition of a diffractive phenomenon. In figure 3b) is shown the distribution of η^*_{max}, the most forward pseudo–rapidity in the $\gamma^* p$ CM frame (where as in the laboratory frame the incident proton direction specifies positive η^*) of any hadronic energy in the LAr. If the rapidity gap implied by the measurement of η^*_{max}, extends right to the forward proton direction, then the lack of any dependence ("exponential suppression") amounts to a diffractive proton interaction à la Bjorken.

The interpretation is that there is a colourless momentum transfer coupling to the incident proton in the DIS ep interaction because of the lack of any significant hadronic energy in the rapidity gap (figure 2b). Assuming the Bjorken criteria, this colourless momentum transfer corresponds to that in diffraction, which is usually discussed in terms of the exchange of a pomeron ($I\!P$) in the parlance of soft hadronic physics. We have a deep–inelastic diffractive $\gamma^* p$ interaction in which the proton scatters or dissociates, leaving itself or most of its dissociation products in the beam pipe. It is thus often convenient to refer to this class of interactions as DIS with a "colourless proton remnant" (hereafter written R_c).

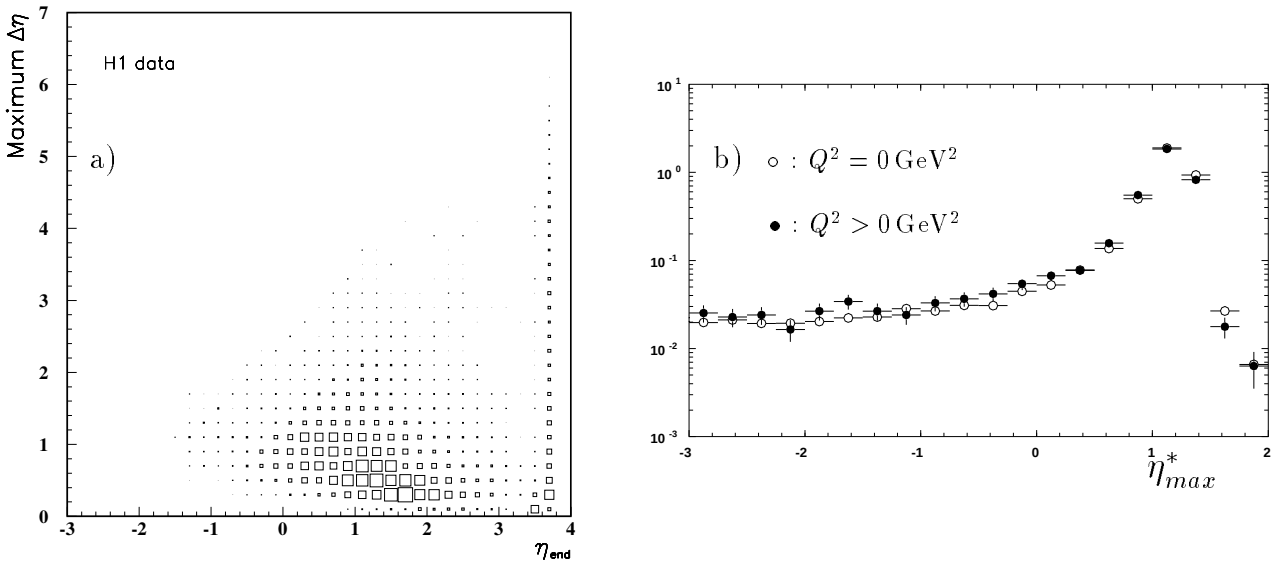

Figure 3: For all ep DIS candidate events, a) scatter plot of the forward end η_{end} of the largest laboratory pseudo–rapidity interval $\Delta\eta$ which is devoid of hadronic energy in the LAr against $\Delta\eta$; a distinct class of events with a tail to large $\Delta\eta$ and with an interval ending at the end of the acceptance of the LAr ($\eta = 3.65$) is visible; b) distribution of maximum pseudo–rapidity η^*_{max} for both ep DIS events (filled points) and ep photoproduction events (open points) in the $\gamma * p$ CM system; the plateau with no exponential suppression corresponding to diffractive interactions is clearly visible in both.

It is also important to realise that the distinction of such a class of DIS interactions in the total DIS sample is solely a matter of being able to define a "leading" remnant R_c as a hadron or collection of hadrons whose sum total of momentum is a large fraction $1 - x_{I\!P} = 1 - x_S$ of the incident proton momentum (see section 3 and section 5 below for the specification of x_S and $x_{I\!P}$). The requirement of a forward rapidity gap devoid of hadronic energy is only one way of quantifying this momentum fraction. An alternative way would be to detect directly R_c or the constituents of R_c as a particle or cluster of particles with a large forward rapidity. In both cases, there exists an interval of rapidity adjacent to R_c in which hadron production is suppressed. This interval defines the constituent or constituents which make up R_c and is the signal which motivates the interpretation that R_c corresponds to colourless momentum transfer coupling to the incident proton. Kinematics requires that as $1 - x_{I\!P}$ decreases the probability of a colourless momentum transfer having such a rapidity gap adjacent to R_c decreases, and inevitably with this decrease the physics distinction between DIS events with and without a colourless remnant R_c disappears.

5 The Contribution of Diffraction to Deep–Inelastic ep Scattering

To proceed further requires a more quantitative approach, and this has been achieved in H1 by evaluating the contribution to the proton structure function F_2 of interactions with colourless exchange coupling to the incident proton. A sample of events in which such a mechanism is likely to predominate is obtained by requiring the presence of a rapidity gap adjacent to the remnant R_c.

The procedure starts with the definition of the quantity to be measured as $F_2^{D(3)}$, which, anticipating the results, is called the "diffractive structure function" following the original procedure of [13, 14]. The measurement of $F_2^{D(3)}$ is made as a function of the three kinematic variables β, Q^2, and x_{Bj}, or equivalently β, Q^2, and $x_{I\!P} = x_S$ (see section 3). In direct analogy

with the definition of F_2 [16], $F_2^{D(3)}$ is evaluated assuming

$$\frac{\mathrm{d}^3\sigma^{ep\to eXR_c}}{\mathrm{d}x_{Bj}\mathrm{d}Q^2\mathrm{d}x_{I\!P}} = \frac{4\pi\alpha^2}{x_{Bj}Q^4}\left\{1-y+\frac{y^2}{2}\right\}F_2^{D(3)}(x_{Bj},Q^2,x_{I\!P}) \tag{5}$$

where there is an implicit integration of the ep DIS cross section $\frac{\mathrm{d}^4\sigma^{ep\to eXR_c}}{\mathrm{d}x_{Bj}\mathrm{d}Q^2\mathrm{d}x_{I\!P}\mathrm{d}t}$ for the process $ep \to eXR_c$ over the unmeasured quantity t, the 4–momentum transfer squared at the incident proton vertex, and where the sensitivity to the longitudinal to transverse virtual photon cross section ratio $\sigma^{\gamma^*_L p\to XR_c}/\sigma^{\gamma^*_T p\to XR_c}$ for rapidity gap dynamics is ignored because its effect is small at the present level of experimental precision. These, and other details, are all discussed in [15].

In terms of the discussion of deep–inelastic kinematics in section 3, the distribution of invariant mass constituting W is here compartmentalised nicely in terms of M_X, which is measured in each event as the invariant mass in LAr to the start of the forward rapidity gap (η_{max}), and the rest, which is associated with the proton remnant R_c in the deep–inelastic process $ep \to eXR_c$ and which is mostly outside the acceptance of the experiment (that is inside the beam pipe). In terms of this M_X, $x_S = x_{I\!P}$ (section 3) becomes the fraction of the incident proton 4–momentum P carried in the colourless exchange, assumed to be a low $|\,t\,|$ phenomenon. Therefore, by requiring that DIS events have an η_{max} and so a well defined mass M_X, a sample is obtained in which for each event three kinematic variables Q^2, x_{Bj} and β (or equivalently Q^2, $x_{I\!P}$ and β) are determined. Furthermore, for these events colour isolation between R_c and the deep–inelastic fragments is most likely because of the isolation in rapidity of R_c which is kinematically implicit in its leading momentum $P_{R_c} = (1-x_{I\!P})\cdot P$. The process, whose cross section is measured and quoted in the form of $F_2^{D(3)}$, then corresponds to $ep \to eXR_c$.

The data used to evaluate $F_2^{D(3)}$formed the sub-set of the sample of deep–inelastic scattering events, which were used to determine the proton structure function F_2 [16], with a forward rapidity gap. DIS events are selected by requiring a scattered electron (positron) with sufficient energy $E' \gtrsim 5\,\mathrm{GeV}$ to trigger in the BEMC and BPC (typical events are shown in 1). Off–line the kinematics are reconstructed using both the scattered e and the hadronic final state [16]. There is redundancy in determining Q^2 from e, and then y from either or both of the scattered e and the hadronic quantity $E_{had} - P_{z\,had}$ which is well measured in the LAr (E_{had} is the total hadronic energy measured and $P_{z\,had}$ its z component) [17]. This facilitates powerful cross checks at many stages of the analysis, in particular concerned with the effects of radiative corrections and with the lack of any good y measurement from the scattered e at low y. The necessary accuracy is achieved by a judicious combination of track measurement in the CTD and energy cluster measurement in the LAr. The final data sample requires $E' \geq 8\,\mathrm{GeV}$ and is selected to be within well understood "fiducial ranges" in Q^2 measured in the BEMC and the LAr. The small level of background from photoproduction processes which can fake a good e tag and survive the kinematic analysis above is quantified by Monte Carlo simulation and comparison with DIS ep candidates which also have energy tagged in LUMI.

The contribution $F_2^{D(3)}$to F_2 attributable to colourless exchange with the proton is then evaluated from the data using DIS events for which a forward rapidity gap, that is an η_{max} cut, can be established. Figure 4a) shows the η_{max} spectrum measured using the LAr energy clusters of all ep DIS data. A "non–exponentially suppressed tail", now in the colinear ep set of reference frames, extending away from the forward direction is clear. The expectation from simulations [18, 19] of ep DIS which do not include any such colourless exchange clearly fails to account for this tail.

In the H1 analysis the forward detectors (see figure 1) PLUG ($3.54 < \eta < 5.08$) and FMD ($5.0 < \eta < 6.6$) play a crucial role because they cover the region where hadron production is

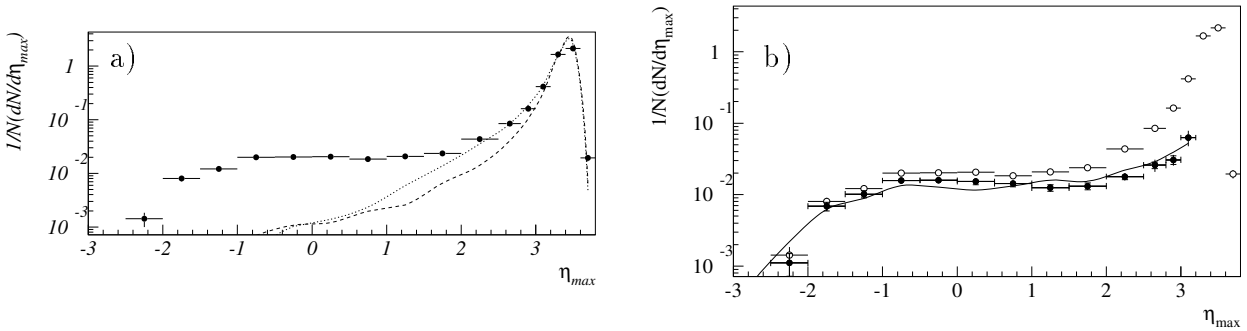

Figure 4: Distribution of maximum pseudo–rapidity η_{max} for ep DIS events; the excess at smaller η_{max} is clearly visible; also shown in a) are the expectations from two "standard DIS" simulations (CDM and MEPS) in which the probing virtual photon couples directly with a quark in the proton; also shown in b) is the η_{max} spectrum of the final data used to evaluate $F_2^{D(3)}$together with the expectation from a diffractive deep–inelastic simulation RAPGAP.

most likely to be depleted for colourless momentum transfer coupling to the proton [5]. As a result they permit a sample of events to be selected with $\eta_{max} = 3.2$ so that almost all of the acceptance of LAr ($\eta \leq 3.65$) is available for subsequent physics analysis. This has two very important consequences for the measurement of $F_2^{D(3)}$. The number of events with a well defined M_X is maximised, and almost the full kinematic range in M_X which can be measured with LAr is available. In figure 4b) the η_{max} distribution is shown for the final sample of putative diffractive events extending to $\eta = 3.2$, together with the expectation of a diffractive DIS simulation [20]. The acceptance of the forward detectors also means that the invariant mass of the colourless remnant R_c can be constrained to be below an upper limit with known efficiency. Also when this acceptance is combined with the η_{max} cut, the momentum transfer variable t is constrained to the range $|t| \lesssim 7\,\mathrm{GeV}^2$.

An apparent problem, which is common to all analyses of this type, is the definition at larger η_{max} values (corresponding to larger M_X and $x_{I\!P}$ values) of the contribution due to "standard DIS" events in which a rapidity gap occurs in the normal course of statistical fluctuation in parton hadronisation. In the H1 analysis, this contribution is estimated as a function of β, Q^2, and $x_{I\!P}$ using the two very different simulations CDM and MEPS (see figure 4), and for the results presented here this contribution is not included in $F_2^{D(3)}$and a conservative error in the subtraction is also included. With the benefit of hindsight since publication and in view of the definition specified above of the measured cross section to which $F_2^{D(3)}$ amounts, it is not appropriate to make this subtraction. However the effect of it on the final results quoted below is not in any way significant at the present level of accuracy.

The whole analysis is repeated for a variety of different cuts in η_{max}, including none whatsoever. Apart from changing somewhat the kinematic range accessible, the results, measured point by measured point, are always completely consistent to well within final errors.

The results for $F_2^{D(3)}$are summarised in figure 5.

6 The Identification of and Characteristics of Diffraction in Deep–Inelastic *ep* Scattering

Everywhere $F_2^{D(3)}$ is observed to decrease monotonically with increasing $x_{I\!P}$ in the measured range $3 \times 10^{-4} \leq x_{I\!P} < 0.05$. An excellent fit to all data points, irrespective of β and Q^2, is obtained assuming a polynomial dependence $x_{I\!P}^{-n}$ with a single exponent $n = 1.19 \pm 0.06(stat.) \pm 0.07(syst.)$, χ^2/d.f. = 32.0/46, 94% C.L. (χ^2/d.f. = 64.5/46, 4% C.L. assuming only statistical errors). The observed universal dependence on $x_{I\!P}$ is thus a feature of the measurements at the

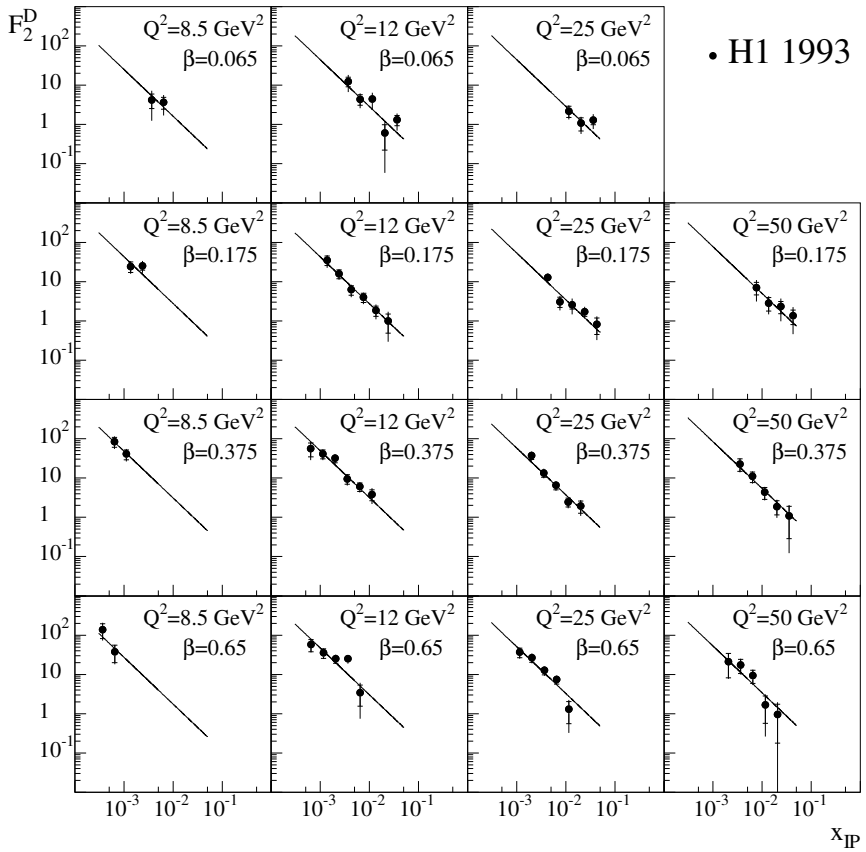

Figure 5: The diffractive contribution $F_2^{D(3)}(\beta, Q^2, x_{I\!P})$ to the proton structure function F_2 as a function of $x_{I\!P}$ for different β and Q^2; the inner error bar is the statistical error; the full error shows the statistical and systematic error added in quadrature; superimposed is the result of the fit establishing a factorisable dependence of the form $\propto x_{I\!P}^{-n}$ (see text). Note that an overall normalisation uncertainty of 8% is not included.

level of statistical accuracy. There is no evidence for any systematic trend in the contributions to χ^2 as a function of β and Q^2.

Such a universal dependence on $x_{I\!P}$, independent of β and Q^2, is expected naively if the deep–inelastic process responsible for rapidity gap events involves a (colourless) target T in the incident proton whose characteristics are not dependent on $x_{I\!P}$, and which carries only a small fraction of the proton's momentum. The dependence of $F_2^{D(3)}(\beta, Q^2, x_{I\!P})$ then factorises into the product of a universal term ($f_{T/p}(x_{I\!P}) \propto x_{I\!P}^{-n}$), which describes the "flux" of T "in" the proton, and a term which describes any structure of T and which is a function of only β and Q^2. The electron scattering cross section for the process $ep \to eXR_c$ can then be written

$$\frac{\mathrm{d}^3\sigma_{ep\to eXR_c}}{\mathrm{d}\beta \mathrm{d}Q^2 dx_{I\!P}} = \frac{\mathrm{d}^2\sigma_{eT\to eX}}{\mathrm{d}\beta \mathrm{d}Q^2} \cdot f_{T/p}(x_{I\!P})$$

where $\frac{\mathrm{d}^2\sigma_{eT\to eX}}{\mathrm{d}\beta \mathrm{d}Q^2}$ describes the deep–inelastic scattering of the electron off T.

The interpretation of the colourless component T of the proton follows from the phenomenology of hadronic physics and the shibboleth of the $I\!P$. The latter arises in the successful encapsulation of the dependences of hadron–hadron interaction cross sections in terms of parameters which specify leading Regge pole exchanges [21, 22, 23]. This Regge phenomenology is also applicable to the virtual photon–hadron process which is of interest here, namely $\gamma^* p \to XR_c$. It includes of course the possibility of diffractive virtual photon–hadron interactions, for which there is no flavour or charge exchange, and the cross sections of which exhibit no decrease with increasing W^2.

In such terms the differential cross section for the process $\gamma^* p \to X R_c$ can be written

$$\frac{\mathrm{d}^2\sigma^{\gamma^* p \to X R_c}}{\mathrm{d}M_X^2 \mathrm{d}t} = f(M_X^2, t) \cdot (W^2)^{2\alpha(t)-2} \tag{6}$$

in the "asymptotic limit", $t/W^2 \to 0$, $M_X^2/W^2 \to 0$ and $Q^2/W^2 \to 0$ (i e $x_{I\!P} \to 0$) and when a single Regge pole exchange with trajectory $\alpha(t)$ provides an adequate description of the cross section. In the above $f(M_X^2, t)$ is some function which depends on the phase space and t dependence (usually peripheral and broadly of the form e^{bt} $b \gg 1$). Thus for a diffractive process with a cross section which is constant or slowly rising with increasing W^2 and which has a peripheral t dependence so that $|\,t\,|$ is small, $\alpha(t) \gtrsim 1$. At fixed M_X^2 and Q^2 (or equivalently at fixed β and Q^2) and with equation 2 it follows that this minimal assumption is equivalent to

$$\frac{\mathrm{d}^2\sigma^{\gamma^* p \to X R_c}}{\mathrm{d}x_{I\!P} \mathrm{d}t} \propto \frac{1}{x_{I\!P}^{2\alpha(t)-1}} \qquad (Q^2/W^2 \to 0) \tag{7}$$

in terms of the $x_{I\!P}$ dependence of the cross section. Employing the relationship between a virtual photon–hadron interaction cross section and the corresponding contribution ($F_2^{D(3)}$) to the proton structure function and then integrating over t gives

$$\frac{\mathrm{d}\sigma^{\gamma^* p \to X R_c}}{\mathrm{d}x_{I\!P}} = \frac{4\pi^2\alpha}{Q^2(1-x_{Bj})} F_2^{D(3)}. \tag{8}$$

So, because the t integration includes what is most likely to be a peripheral dependence of the cross section $\frac{\mathrm{d}^2\sigma^{\gamma^* p \to X R_c}}{\mathrm{d}x_{I\!P}\mathrm{d}t}$ and a slow dependence of $\alpha(t)$, $F_2^{D(3)}$is also expected to exhibit something close to this polynomial $x_{I\!P}$ dependence. Thus the characteristic slowly rising W^2 dependence of a diffractive process translates into a falling $x_{I\!P}$ dependence of the form $x_{I\!P}^{-n}$, $n \gtrsim 1$.

If T is taken to be well parameterised in terms of "Reggeised" hadronic exchanges, then the $x_{I\!P}$ dependence of the flux factor in equation 6 is specified by the trajectory of the leading Regge exchange $\alpha(t)$ in the "asymptotic limit" $x_{I\!P} \to 0$, $t/W^2 \to 0$. The dependence takes the form of equation 7. In this measurement we perforce integrate over t. As a first approximation, $\alpha(t)$ may be replaced by $\alpha_{t=0}$ because the t distribution of the soft hadronic proton interaction is likely to be peripheral and the t dependence of $\alpha(t)$ is likely to be slight.

In this approximation the observed $x_{I\!P}$ dependence is consistent with the leading (effective) trajectory which describes phenomenologically "soft hadronic" diffractive interactions, namely the $I\!P$ with $\alpha(t) = \alpha_{t=0} + \alpha' t$ and $\alpha_{t=0} = 1.085$, $\alpha' = 0.25\,\mathrm{GeV}^{-2}$ [24]. The colourless proton remnant R_c is then either a proton or an isospin $\frac{1}{2}$ baryon excitation (eg N^*, $N^*\pi$, etc). If the t dependence of proton diffraction is here like that in soft pp collisions, namely peripheral with $b \gg 1$ in a dependence e^{bt}, then the systematic error, which arises by ignoring any t dependence of $\alpha(t)$ when taking $n = 2\alpha_{t=0} - 1$, does not exceed $\sim +4$ to $+5\%$ of $\alpha_{t=0}$ (assuming that the slope α' of the $I\!P$ trajectory is $0.25\,\mathrm{GeV}^{-2}$). Note that the leading meson Regge trajectories, the $f_2(1270)/\omega(783)$ for a diffractive–like process with no isospin exchange, and the exchange degenerate $\rho(770)/a_2(1320)$ for a process involving isospin exchange, have intercept $\alpha_{t=0} \sim 0.5$, giving rise to an $x_{I\!P}$ dependence which is much less steep. Parameterisations of pion exchange, either "Reggeised" ($\alpha_{t=0} \sim 0$) or otherwise, have only a slight dependence on $x_{I\!P}$. Therefore the interpretation of the rapidity gap events in DIS at low Bjorken–x as being due in the main either to diffractive scattering or to diffractive dissociation of the incident proton can be made without ambiguity.

It is worth pointing out that the use of Regge Pole phenomenology in the above discussion of $F_2^{D(3)}$and deep–inelastic diffraction has been solely to provide a template with which to

compare with hadron–hadron diffraction. This template assumes no more than the polynomial parametrisation in equation 6 of the W^2 dependence of a high energy $\gamma^* p$ interaction cross section, following its successful use in diffractive and other hadron–hadron physics. None of the conclusions concerning the dominance of a diffractive proton interaction and the lack of any evidence for a significant non–diffractive contribution depend on more than the use of this polynomial parametrisation to quantify the W^2, or equivalently the $x_{I\!P}$, dependence of the measured cross section in the form of $F_2^{D(3)}$. It is interesting to note that such a parametrisation can be justified theoretically even without resort to the Regge representation of a high energy scattering amplitude on the sole basis of the analyticity of scattering amplitudes [26]. Experimentally of course its use is justified in that it describes well the gross feature of the W^2 dependences of cross sections which distinguish diffractive from other hadron–hadron interactions.

7 The Hard $I\!P$ and Deep–Inelastic Diffraction

Since the advent of QCD as the theory of the strong interactions, attempts have been made to confront it with the bulk, rather than the perturbative "p_T tail" at short distance, of the cross section for the interaction of two hadrons. In calculations which use the BFKL QCD formalism of $I\!P$ dynamics, calculations of qq diffraction have been achieved in which the low p_T divergences implicit in multi–gluon exchange can be treated in a plausible way, and which then give rise to a Regge asymptotic form. The resulting $I\!P$ is found to be "hard" with an intercept $\alpha_{t=0} = 1 + \varepsilon$, $\varepsilon \lesssim 0.5$ [25, 27]. It is therefore worthwhile to take the minimal Regge parametrisation, as encapsulated in equation 6 and then applied to the measurements of $F_2^{D(3)}$ in section 6 above, at face value, and to compare the results for the leading Regge trajectory $\alpha(t)$ with this BFKL expectation.

Combining in quadrature the statistical and systematic errors of the measurement of the $x_{I\!P}$ dependence above, the intercept cannot exceed 1.25 (i.e. $\varepsilon \leq 0.25$) with 99.85% confidence, if the effects of the t integration of equation 7 are ignored. The simplest, but debatable, assumption concerning t dependence (based as above on a trajectory slope $\alpha' = 0.25\,\mathrm{GeV}^{-2}$, on a peripheral t dependence of the cross section, and on a plausible proton dissociation mass spectrum) could raise this upper limit by between 0.04 and 0.05. Thus this measurement does not rule out the existence of a "hard" BFKL $I\!P$, especially if it contributes together with a soft component, such as that described above. A recent calculation, also based on a BFKL approach, suggests also that the simplest factorisation with an $x_{I\!P}$ dependence $\propto x_{I\!P}^{-n}$ may not strictly hold [28]. The accuracy of this measurement of the $x_{I\!P}$ dependence does not exclude such a possibility.

An alternative, but equivalent, way of demonstrating the nature of the $I\!P$ in a diffractive process, and thereby searching for evidence of a hard perturbative contribution, is to revert to the W^2, rather than $x_{I\!P}$, dependence of the interaction cross section. Furthermore, in DIS at low Bjorken–x, the W^2 dependence amounts to the x_{Bj} dependence (equation 1), and equation 6 is equivalent to

$$\frac{\mathrm{d}^2\sigma^{\gamma^* p \to X R_c}}{\mathrm{d}M_X^2 \mathrm{d}t} \propto \frac{f(M_X^2, t)}{x_{Bj}^{2\alpha(t)-2}}. \tag{9}$$

Thus any W^2 dependence of a hadronic virtual photon interaction cross section, here $\gamma^* p \to X R_c$ (at fixed M_X^2), specifies directly the x_{Bj} dependence at fixed Q^2 of the cross section, and, using equation 8, also of $F_2^{D(3)}$.

The x_{Bj} dependence of $\frac{\mathrm{d}^2\sigma^{\gamma^* p \to X R_c}}{\mathrm{d}M_X^2 \mathrm{d}t}$ at fixed Q^2 and fixed M_X^2 (that is fixed β) can be compared directly with the x_{Bj} dependence of the total DIS cross section $\sigma^{\gamma^* p \to X}$ at the same Q^2. The

latter is of course now well measured in the form of the x_{Bj} dependence (figure 6) of the proton structure function F_2 [16]. It demonstrates a notable increase as x_{Bj} decreases, corresponding to an increase of $\sigma^{\gamma^* p \to X}$ with increasing W^2 (using the relation analogous to equation 8 for F_2 in terms of $\sigma^{\gamma^* p \to X}$). Using the optical theorem to relate this total cross section to the forward elastic, and therefore diffractive, scattering amplitude for the process $\gamma^* p \to \gamma^* p$, Regge phenomenology yields the expression

$$\sigma^{\gamma^* p \to X}(W^2, Q^2) \propto (W^2)^{\alpha_{t=0}-1}$$

or equivalently

$$\sigma^{\gamma^* p \to X}(x_{Bj}, Q^2) \quad \propto \quad \frac{1}{x_{Bj}^{\alpha_{t=0}-1}} \qquad (\frac{Q^2}{W^2} \to 0) \tag{10}$$

for this x_{Bj} dependence. The rise of F_2 is again governed by the trajectory, but this time only the intercept $\alpha_{t=0}$. Numerical parametrisations of the (x_{Bj}, Q^2) dependence of F_2 show that the rise is well parametrised by a leading dependence $\propto x_{Bj}^{-m}$ with $m \sim 0.19$ to 0.25 [16]. Thus the behaviour of the x_{Bj} dependence of the proton structure function F_2 can be taken as evidence for a "harder" $I\!P$ with $\varepsilon = \alpha_{t=0} - 1 \sim 0.19$ to 0.25 in high Q^2 virtual photon Compton scattering. However it is here worth noting that these measurements of F_2 are well described by a conventional DGLAP QCD fit [29], so whether the rise with decreasing x_{Bj} can be interpreted as a "harder" $I\!P$ in the theoretical sense of BFKL is unclear.

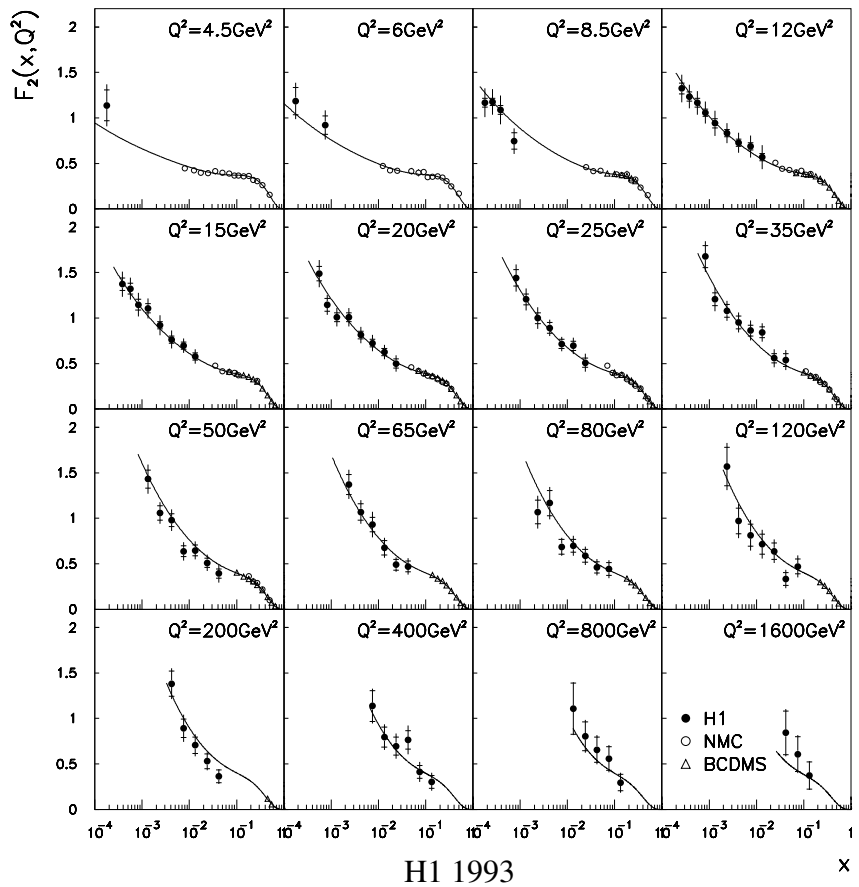

Figure 6: The proton structure function F_2 as a function of Bjorken–x at fixed Q^2; superimposed on the x_{Bj} dependence is the result of a NLO DGLAP QCD fit.

A comparison of the x_{Bj} dependences of $\frac{\mathrm{d}^2\sigma^{\gamma^* p \to X R_c}}{\mathrm{d}M_X^2 \mathrm{d}t}$ and $\sigma^{\gamma^* p \to X}$ therefore becomes a comparison of the manifestations of the $I\!P$ in deep–inelastic scattering and deep–inelastic diffraction.

In H1 such a comparison has been made [30] in the form of a measurement of the quantity

$$r^{D(3)}(x_{Bj},Q^2) = \frac{\mathrm{d}^3\sigma^{ep\to eXR_c}}{\mathrm{d}x_{Bj}\mathrm{d}Q^2\mathrm{d}\beta} \Big/ \frac{\mathrm{d}^2\sigma^{ep\to eX}}{\mathrm{d}x_{Bj}\mathrm{d}Q^2} = \frac{x_{Bj}}{\beta^2}\cdot\frac{F_2^{D(3)}(\beta,x_{Bj},Q^2)}{F_2(x_{Bj},Q^2)} \tag{11}$$

where the extra factor $\frac{x_{Bj}}{\beta^2}$ arises because of the Jacobian between the defining equation 5 for $F_2^{D(3)}$and the dependence which is now of interest, namely on x_{Bj} at fixed Q^2 and β.

The result is shown in figure 7. At different β and Q^2 there is no significant evidence yet for any differences between the observed x_{Bj} dependences of the cross sections for deep–inelastic diffraction and deep–inelastic scattering. The x_{Bj} dependence of the deep–inelastic diffractive cross section is thus consistent with the rise with decreasing x_{Bj} of the deep–inelastic scattering cross section (that is of F_2), namely $\propto x_{Bj}^{-m}$ with $m \sim 0.19$ to 0.25. However the experimental precision is limited due to the accuracy of this first measurement of $F_2^{D(3)}$– superimposed is a best fit of a universal dependence $r^{D(3)} \propto x_{Bj}^{-m}$ for which $m = -0.06 \pm 0.06(\mathrm{stat.}) \pm 0.08(\mathrm{syst.})$.

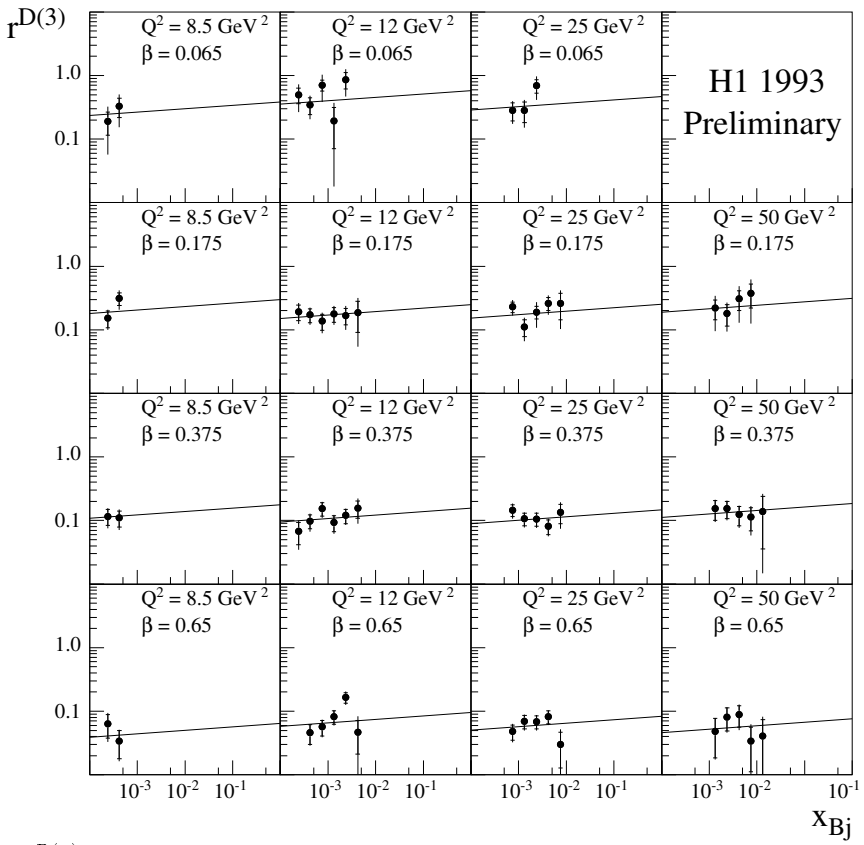

Figure 7: Ratio $r^{D(3)}(\beta,x_{Bj},Q^2)$ (see text) which compares the x_{Bj} dependences of the deep–inelastic diffractive cross section $\mathrm{d}^3\sigma^{ep\to eXR_c}/\mathrm{d}x_{Bj}\,\mathrm{d}Q^2\mathrm{d}\beta$ with the total cross section $\mathrm{d}^2\sigma^{ep\to eX}/\mathrm{d}x_{Bj}\mathrm{d}Q^2$.

Interpreting the result in figure 7 in terms of the manifestation of the $I\!P$ in deep–inelastic diffraction (DIF) and in deep–inelastic scattering (DIS) requires the use of equations 9 and 10 to specify (in obvious notation)

$$r^{D(4)}(\beta,x_{Bj},Q^2,t) \propto \frac{1}{x_{Bj}^{2\alpha_{DIF}(t)-2-\varepsilon_{DIS}}}$$

in which distinction is made between the $I\!P$ trajectories of DIF and DIS. If the effect of the t integration (as in equation 7 to give equation 8) is ignored, that is if any "shrinkage" is ignored so that $\varepsilon_{DIF} = \alpha_{DIF\,t=0} - 1 \approx \alpha_{DIF}(t) - 1$, then

$$r^{D(3)}(\beta,x_{Bj},Q^2) \propto \frac{1}{x_{Bj}^{2\varepsilon_{DIF}-\varepsilon_{DIS}}}. \tag{12}$$

The presence or not of any shrinkage depends on the t dependence of $\alpha(t)$. Its effect on this expression for $r^{D(3)}$ depends also on the t dependence of the cross section $\frac{\mathrm{d}^4\sigma^{ep\to eXR_c}}{\mathrm{d}x_{Bj}\mathrm{d}Q^2\mathrm{d}\beta\mathrm{d}t}$, or equivalently $\frac{\mathrm{d}^2\sigma^{\gamma^* p\to XR_c}}{\mathrm{d}\beta\mathrm{d}t}$. Perturbative BFKL calculations of the $I\!P$ seem to find little or no dependence of α on t, and thus little or no modification to equation 12. As mentioned above, hadron phenomenology finds $\alpha' = 0.25\,\mathrm{GeV}^{-2}$ [24], and thus a correction which, for a given ε_{DIF}, will reduce the significance of the falling(rising) dependence on $x_{Bj}(W^2)$.

At fixed β the sensitivity of the x_{Bj} dependence of $F_2^{D(3)}$to ε_{DIF} is thus roughly twice that of the x_{Bj} dependence of F_2 to ε_{DIS}. Always with the complications for equation 12 of shrinkage in mind, the description in terms of a universal dependence $r^{D(3)} \propto x_{Bj}^{-m}$ is equivalent to $\varepsilon_{DIF} \approx \varepsilon_{DIS}/2 - 0.03 \pm 0.03(\mathrm{stat.}) \pm 0.04(\mathrm{syst.})$. Given that the x_{Bj} dependence of F_2 corresponds to $\varepsilon_{DIS} \sim 0.19$ to 0.25 (see above), then $\varepsilon_{DIF} \approx 0.07$ to $0.10 \pm 0.03(\mathrm{stat.}) \pm 0.04(\mathrm{syst.})$. Thus it is not yet possible to conclude that the $I\!P$ in DIF is "softer" than, or as "hard" as, it seems to be in DIS until the accuracy of the measurements of $F_2^{D(3)}$improve and their scope includes t dependence. Of course this conclusion is just a restatement of that above based on the analysis of DIF in terms of the $x_{I\!P}$ dependence of $F_2^{D(3)}$. But now the comparison is made using the Compton scattering interpretation of the x_{Bj} dependence of F_2 as template for a "harder" $I\!P$.

Thus the identification of any contribution to deep–inelastic diffraction which may be attributed to a "hard" BFKL–like $I\!P$ contribution requires more accurate measurements of $F_2^{D(3)}$and a careful analysis of them using the appropriate Regge phenomenology. This is much along the lines of what has been done with the wealth of diffractive hadronic physics data [24], but also now with the added spice of a hard probing virtual photon and the perturbative QCD implications which are described in section 9 below.

8 The Total Contribution of Proton Diffraction to Deep–Inelastic *ep* Scattering

The measurement of $F_2^{D(3)}$has been used to determine the total contribution of diffraction to F_2 as a function of x_{Bj} and Q^2. Diffraction is defined to be for $x_{Bj} \le x_{I\!P} \le 0.05$ so that the contribution can be expressed as $F_2^D(x_{Bj}, Q^2)$ which is related to $F_2^{D(3)}$according to

$$F_2^D(x_{Bj}, Q^2) = \int_x^{0.05} F_2^{D(3)}(x_{Bj}, Q^2, x_{I\!P})\mathrm{d}x_{I\!P} \tag{13}$$

The results are shown in figure 8, both as $F_2^D(x_{Bj}, Q^2)$ and as the proportion $r^D(x_{Bj}, Q^2) = F_2^D/F_2$. Note that both F_2^D and r^D tend to zero as $x_{Bj} \to x_{I\!P}$. Away from this kinematic limit, r^D is rather insensitive to x_{Bj} and Q^2 and is about 10% [4].

Either $F_2^D(x_{Bj}, Q^2)$ or $r^D(x_{Bj}, Q^2)$ quantify the total contribution to deep–inelastic ep scattering due to proton diffraction. The interesting question which now arises is exactly how this diffractive contribution should be taken into account in DGLAP (or otherwise) based QCD analyses of the proton structure function F_2 at low x_{Bj} and the extraction of parton distribution functions (pdf's) of the proton [29]. There as yet seems to be no conclusive answer [31, 32].

[4]Note that the x_{Bj} dependence of $F_2^D(x_{Bj}, Q^2)$ does *not* have as straighforward an interpretation in terms of the nature of the $I\!P$ in deep–inelastic diffraction as does $r^{D(3)}$ because $F_2^D(x_{Bj}, Q^2)$ does not correspond to the differential cross section $\frac{\mathrm{d}^2\sigma^{\gamma^* p\to XR_c}}{\mathrm{d}M_X^2\,\mathrm{d}t}$, or integration of it over t, and thereby to its parametrisation as in equation 6.

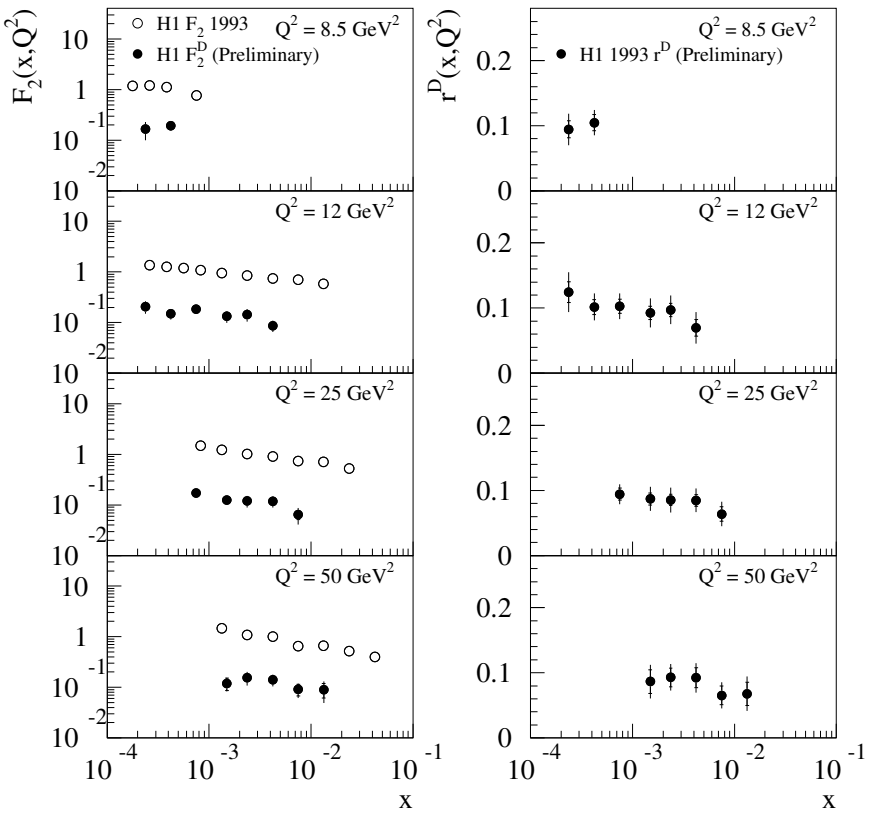

Figure 8: The structure function $F_2^D(x_{Bj}, Q^2)$ and the ratio $r^D = F_2^D(x_{Bj}, Q^2)/F_2(x_{Bj}, Q^2)$ for $x_{I\!P} < 0.05$; the result is for deep–inelastic diffraction in which the proton does not dissociate; about a third of deep–inelastic diffractive interactions are consistent with proton dissociation.

9 The Partonic Structure of Proton Diffraction

The observation that rapidity gap events in DIS are dominantly of a diffractive nature, and the evidence for a simple factorisation of the structure function $F_2^{D(3)}(\beta, Q^2, x_{I\!P})$ lead naturally to the interpretation of the β and Q^2 dependence of $F_2^{D(3)}$ as a measure of the deep–inelastic structure of diffractive exchange. If such exchange is taken phenomenologically to be described by an effective Regge trajectory, this interpretation amounts to the deep–inelastic structure of the $I\!P$.

In figure 9 are shown the β and Q^2 dependences of the integral

$$\tilde{F}_2^D(\beta, Q^2) = \int_{x_{I\!P_L}}^{x_{I\!P_H}} F_2^{D(3)}(\beta, Q^2, x_{I\!P})\, \mathrm{d}x_{I\!P},$$

which, assuming factorisation, is proportional to the structure function of the $I\!P$. The range of integration, $x_{I\!P_L} = 3 \times 10^{-4}$ and $x_{I\!P_H} = 0.05$ is chosen to span the entire $x_{I\!P}$ range of measurements of $F_2^{D(3)}$. $\tilde{F}_2^D$ is evaluated assuming that the factorisation hypothesis with the measured dependence on $x_{I\!P}$ is a good description over this range of integration. It is convenient to define $\tilde{F}_2^D(\beta, Q^2)$ in this way to avoid the need to specify the normalisation of the unknown diffractive, or $I\!P$, "flux" in the proton when presenting the data in a form which is suitable for direct comparison with theoretical expectation for $I\!P$ structure.

There is no evidence for any substantial Q^2 dependence of $\tilde{F}_2^D$ for any β. Deep (high Q^2) diffractive interactions are thus broadly of a scale invariant, and therefore point-like, nature. Furthermore, $\tilde{F}_2^D$ is observed to have little dependence on β with contributions throughout the measured range ($0.065 < \beta < 0.65$). Therefore the structure which is resolved by the electron in the high Q^2 diffractive interaction carries only a fraction of the $I\!P$'s momentum, implying

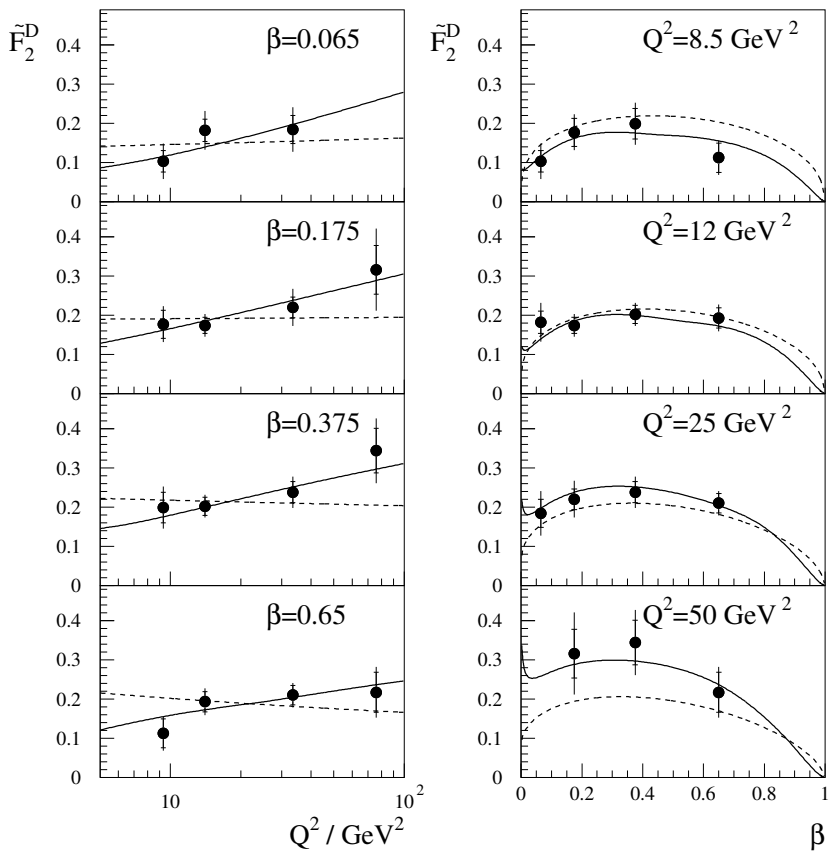

Figure 9: Dependence of $\tilde{F}_2^D$ on Q^2 and β; superimposed are the results of two LO $\log Q^2$ DGLAP QCD fits. The dashed line shows a fit in which at the starting scale, $Q_0^2 = 4\,\mathrm{GeV}^2$, diffraction is attributed to the exchange of only quarks (χ^2/dof of 13/12, 37%C.L.). The solid line shows a fit in which both quarks and gluons may contribute to the diffractive mechanism at $Q_0^2 = 4\,\mathrm{GeV}^2$ (χ^2/dof = 4/9, 91%C.L.). In the latter, the gluons carry $\sim 90\%$ of the momentum of the pomeron at $Q_0^2 = 4\,\mathrm{GeV}^2$.

that the $I\!P$ has its own point-like, presumably partonic, sub–structure.

A fit to the hypothesis of a linear $\log_{10} Q^2$ dependence of the form

$$\tilde{F}_2^D(\beta, Q^2) = a(\beta) \log_{10} Q^2 + b(\beta) \tag{14}$$

yields values for $a(\beta)$ that are $\simeq 1.5\sigma$ above zero for all values of β. The errors in $a(\beta)$ amount to $\sigma = 0.09\,(\log_{10}\,\mathrm{GeV}^2)^{-1}$ for all β except that at $\beta = 0.065$ for which $\sigma = 0.15\,(\log_{10}\,\mathrm{GeV}^2)^{-1}$. Therefore the accuracy of this first measurement of the Q^2 dependence of $\tilde{F}_2^D$ is such that the possibility of "scaling violations", symptomatic of QCD, may be admitted.

The hypothesis that any violation of scale invariance is in the form of a $\log Q^2$ dependence of $\tilde{F}_2^D$ which is independent of β (slope parameter a in equation 14 now independent of β) provides an excellent description of $\tilde{F}_2^D$ and gives $a = 0.14 \pm 0.04$. In this and all subsequent fits below, statistical and systematic errors are added in quadrature.

The lack of any fall of $\tilde{F}_2^D$ with increasing Q^2 at large β contrasts with the violations of scale invariance exhibited by the structure function of a typical hadron. For example, the proton structure function F_2 rises with increasing Q^2 for $x \lesssim 0.15$, and falls with increasing Q^2 for $x \gtrsim 0.15$ [33, 34]. This decreasing dependence at high x is an inevitable consequence of DGLAP QCD evolution for an object with a structure built from the evolution of "valence" quarks in which the latter predominate at large Bjorken–x. By analogy, a structure function for which any violation of scale invariance amounts to an increase with $\log Q^2$ at high Bjorken–x (β),

is likely to have a large gluon, relative to quark, content in its valence parton density. The observation that the Q^2 dependence of $\tilde{F}_2^D$ is consistent with a rise proportional to $\log Q^2$ thus suggests that a significant contribution to the structure of diffractive exchange is gluonic.

To quantify any substantive evidence for a gluonic contribution to the structure of diffractive exchange, that is to $\tilde{F}_2^D$, the DGLAP evolution equations were solved numerically in LO and in NLO $\log Q^2$ approximations. The numerical technique used followed that of [36] in which, starting from a scale $Q_0^2 = 4\,\mathrm{GeV}^2$, the assumed forms $z^a(1-z)^b$ for the gluon and flavour singlet quark parton densities ($z = x_{i/I\!P}$, quark $i = q$, gluon $i = g$) in diffractive exchange were evolved to higher Q^2 and compared with the measurements of the β dependence of $\tilde{F}_2^D$. The basic kinematic features of the method, for example the treatment of charm, were identical to those in the QCD analysis of the proton structure function F_2 [29]. More details can be found in [37]. In particular, no momentum sum rule was imposed because it is far from clear whether one should exist for such a space–like exchange, and because the normalisation of $\tilde{F}_2^D$ does not coincide with the normalisation of the structure function of diffractive exchange without further theoretical input.

The results of the QCD analysis (figure 9) are only indicative because of the limited precision of this first measurement of $F_2^{D(3)}$ [37]. Nevertheless a picture begins to emerge which confirms the qualititative statements above concerning the $\log Q^2$ dependence at higher β. The measurements favour the presence of a significant gluon contribution (usually between about 70 to 90%) of the form $zg(z) = z^8(1-z)^{0.3}$ ($z = x_{g/I\!P}$) at the starting scale $Q_0^2 = 4\,\mathrm{GeV}^2$ if they are not to exhibit a falling $\log Q^2$ dependence at high β (91% CL). Taking only quarks at $Q_0^2 = 4\,\mathrm{GeV}^2$ with a similar pdf dependence $zq(z) = z^{0.35}(1-z)^{0.35}$ ($z = x_{q/I\!P}$), though acceptable quantitatively (37% CL), does not reproduce this striking feature in the data. Furthermore, and with marginal significance, the favoured gluon distribution in diffractive exchange has the leading form above in which the majority of the diffractive 4–momentum transfer is taken by a single gluon, that is $I\!P$ exchange involves a leading gluon exchange (figure 10a).

An interesting feature of the QCD fit is that a significant contribution to $\tilde{F}_2^D$ from charm is necessary [37], much as expected from a flavour singlet hadronic system such as the $I\!P$. This motivates a search in the diffractive final state for a resonant signal, and sure enough preliminary evidence for charm production is seen when one follows the by now standard recipe using charged particles in the final state (figure 10b). The quantification of this yield in terms of a production cross section is not yet complete.

The observation above that the scaling violations of $\tilde{F}_2^D$ are consistent at the present rather limited level of experimental precision with the form of equation 14 with $a(\beta)$ constant is reminiscent of the dependence of the structure function F_2^γ of the photon [38, 39, 40]. There the observed scaling violations are observed to be consistent with QCD expectation driven by the so–called "inhomogeneous" term which corresponds to the leading "point-like" coupling of the photon to $q\bar{q}$ [41]. Furthermore, such a leading "point–like" coupling has a dependence on the appropriate Bjorken–x like variable which persists to large values by virtue of the $\gamma \to q\bar{q}$ splitting function $P_{q/\gamma} \propto z^2 + (1-z)^2$ contribution $zP_{q/\gamma}$ to F_2^γ. The similarity of F_2^γ with the observed Q^2 and β dependences of $\tilde{F}_2^D$ is striking. The intriguing possibility therefore exists that, like the photon, diffractive exchange ($I\!P$) has such an inhomogeneous, and therefore point–like, contribution to its structure function. In view of the same z dependences of the splitting functions $\gamma \to q\bar{q}$ and $g \to q\bar{q}$, this point–like contribution may naturally be attributed to a gluon. If it is, then any distinction between such a possibility and the more straightforward consequences described above of the application of DGLAP, which seem to show some suggestion of a leading gluon, is unclear. If it is not, then we have something in diffractive exchange which is point–like and which is completely new!

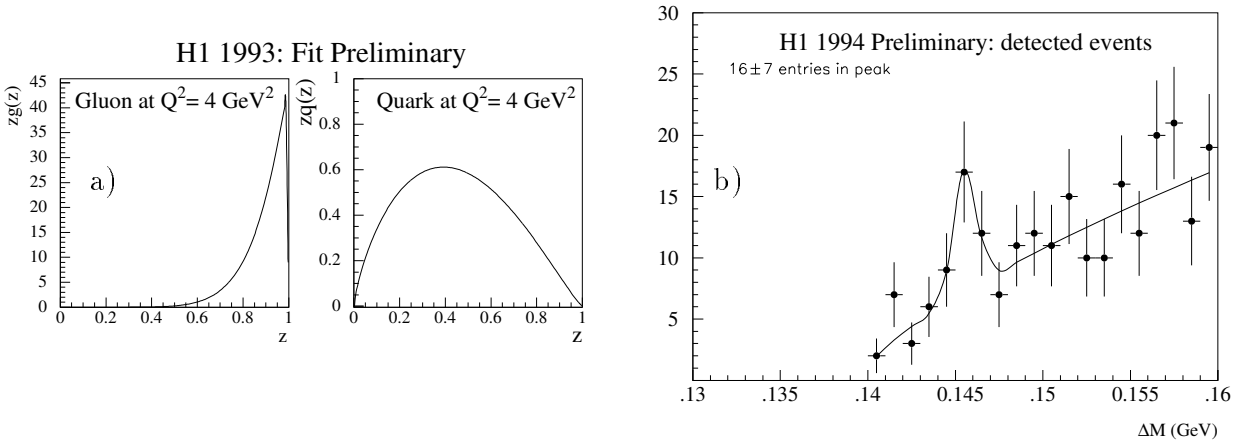

Figure 10: a) The quark flavour–singlet $zq(z)$ and the gluon $zg(z)$ densities at the starting scale $Q_0^2 = 4\,\mathrm{GeV}^2$ in the LO QCD description of $\tilde{F_2^D}$ described in the text in which the lack of any evidence for a decrease with increasing $\log Q^2$ at high β is well described. The gluons account for $\sim 90\%$ of the total momentum in diffractive exchange. The normalisation is specified by the measurement of $\tilde{F_2^D}$ which itself is proportional to the structure function of diffractive exchange. No errors are quoted because they are large enough to mean that a flat density $zg(z)$ is also acceptable; b) the invariant mass combination $\Delta M = M(K^{\pm}\pi^{\mp}\pi^{\mp}_{slow}) - M(K^{\pm}\pi^{\mp})_{D^0}$ in diffractive deep–inelastic scattering events showing evidence for $D^{*\mp}$ production.

10 A Parton Model Approach to Rapidity Gap Physics

Diffraction in terms of $I\!P$ exchange requires a certain faith in the interpretation of the energy dependence of hadronic physics cross sections in terms of a leading effective Regge pole. An attempt has been made by Buchmüller and Hebecker [42] to develop a partonic model of DIS ep events with a rapidity gap without the assumption of any diffractive paradigm, and with the assumption that the underlying partonic process is electron–gluon scattering. The motivation is derived from the importance of such dynamics in low–x_{Bj} deep–inelastic ep scattering, and by implication therefore it requires diffractive exchange to be predominantly a leading gluon phenomenon. It is hypothesised that the quark–antiquark pair produced in the hard electron–gluon interaction undergoes colour rotation so that the colour quantum numbers of the initial quark–antiquark system are completely randomised. Then the probabilities of obtaining a colour singlet or octet configuration in the final state are simply $\frac{1}{9}$ and $\frac{8}{9}$ respectively. When the quark–antiquark pair emerge in a colour singlet state, there is no longer any colour connection between it and the proton remnant, and so a "rapidity gap" is likely. The qualitative features of diffraction in a picture like this, which is driven in essence by (virtual photon) Bethe–Heitler $q\bar{q}$ pair production, has also been pointed out by Kowalski and Ellis [43].

The immediate prediction that $\frac{1}{9}$th of the deep–inelastic ep cross section should be what we hitherto have called proton diffraction is nicely born out in the measurement of $r^D \approx 10\%$ (section 8 above). The approach also leads to a simple, parameter free, prediction for the relationship between the structure functions $F_2(x_{Bj}, Q^2)$ and $F_2^{D(3)}$. A simple scaling law of the form

$$F_2^{D(3)}(\beta, Q^2, x_{I\!P} = \xi) = 0.04 \cdot \frac{F_2(x_{Bj} = \xi, Q^2)}{\xi}$$

is predicted which should hold for any β to the extent that the model predicts little or no β dependence of $F_2^{D(3)}$. This prediction is shown to be broadly correct in figure 11 in which the measurements of $F_2^{D(3)}$for different β are included. The factor 0.04 corresponds to the proportion r^D overall of deep–inelastic diffraction being $\frac{1}{9}$.

The approach of Buchmüller and Hebecker [42] is thus in remarkable agreement with experiment, given the simplicity of this first model calculation. It adds weight to the picture in

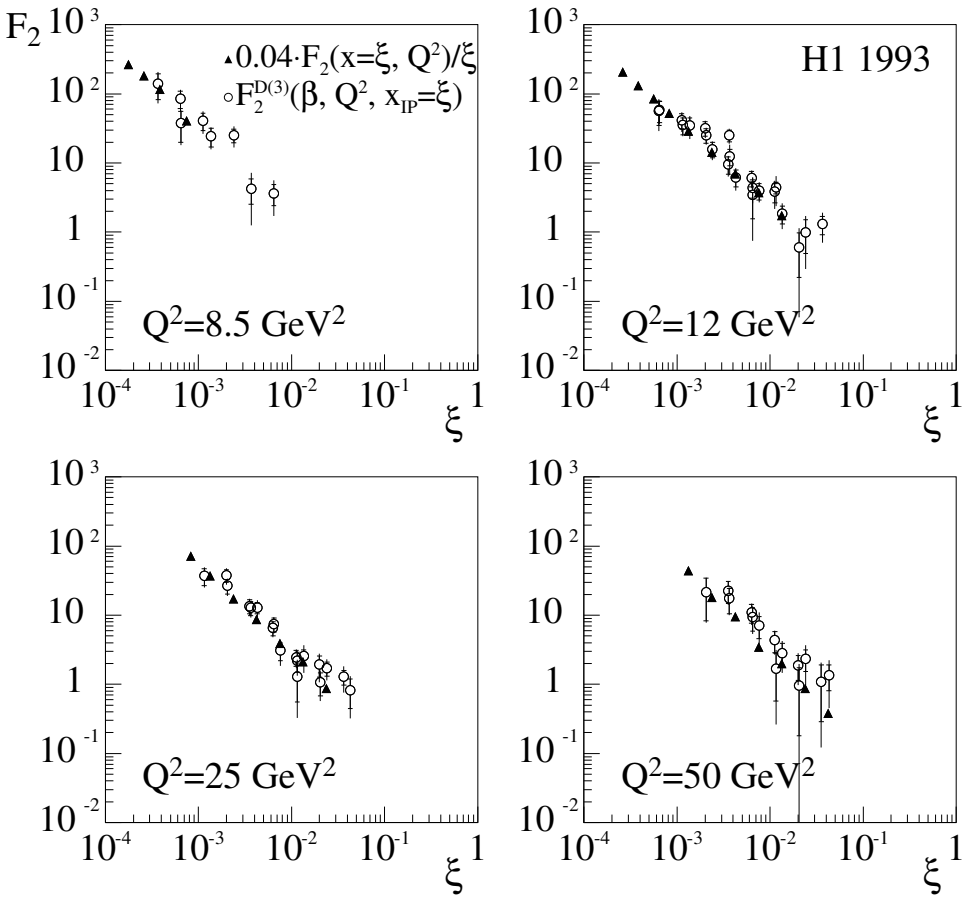

Figure 11: The quantities $F_2^{D(3)}(\beta, Q^2, x_{I\!P} = \xi)$ and $0.04 \cdot F_2(x = \xi, Q^2)/\xi$ as a function of ξ for different values of Q^2 to test the scaling law of Buchmüller et al. (see text); note that the $F_2^{D(3)}$are plotted in each plot for different β.

which diffractive exchange, and thus the $I\!P$, is a leading gluon phenomenon.

11 Conclusion and Outlook

Remarkable progress has been made in our understanding of rapidity gap phenomena in ep DIS since their observation in the first data taken at HERA in 1992. Following quantification in terms of a diffractive structure function $F_2^{D(3)}$, rapidity gap events in ep DIS are now unquestionably attributable to diffractive interactions and amount to roughly 10% of low x_{Bj} ep DIS, irrespective of x_{Bj} ($\ll x_{I\!P}$) and Q^2. To within present experimental uncertainty, the characteristics of the colourless exchange are universal and follow the broad expectation encapsulated in $I\!P$ phenomenology of hadronic diffraction. The deep–inelastic evolution of $F_2^{D(3)}$is readily interpreted in terms of diffraction as a leading gluon phenomenon in QCD.

The next year should see experimental precision improve to the extent that the precise nature of diffractive deep–inelastic dynamics may become established, in particular whether there is real evidence for a "hard" perturbative $I\!P$, anticipated for so long in QCD.

Looking further into the future is yet more exciting. These measurements at HERA amount to nothing less than a revolution in the development of our quantitative understanding of hadronic physics. Each new energy regime of lepton–nucleon physics has been seminal to major advances in our understanding of hadronic structure and interaction. Measurements at the fixed target experiments at SLAC, Fermilab and CERN demonstrated unambiguously

both the quark and gluon structure of nucleons and that QCD is *the* theory of the strong interactions. However, in subsequent decades, we have singularly failed to achieve a quantitative understanding of the bulk of the cross section for the interaction of two hadrons in terms of QCD. The immense increase of the lepton–nucleon CM energy at HERA, with the concomitant access to the low x_{Bj} region of deep–inelastic scattering, mean that we can probe experimentally not just the details of proton sub–structure in this new gluon dominated region, but now for the first time also the partonic structure of the totality of proton–hadron interactions. These first measurements already throw new light on the dominant diffractive component. Subsequent measurements promise a wealth of new insight, and thus can be expected to have a major impact on our understanding, both of the stability or otherwise of hadronic systems, and of their mutual interactions.

Acknowledgements

Je remercie tous les organisateurs de la Rencontre intéressante de Blois 1995 et de l'opportunité pour un séjour agréable au Château de Blois.

None of the physics presented here would have been possible without the immense efforts of very many people. The operation of HERA is due to the dedication and skill of the few who constitute the machine groups at DESY. The construction and operation of H1 is due to similar dedication, skill and determination of technicians and engineers in all the H1 collaborating institutes since 1986. The on–going operation, data taking, and data analysis work is in the expert hands of all my colleagues in H1, with whom it is always a pleasure to work. The support of the UK Particle Physics and Astronomy Research Council is gratefully acknowledged. I thank the DESY laboratory for their hospitality, and the University of Liverpool for maintaining its belief in the merits of a strong and well funded Department of Physics. J. Bartels, W. Buchmüller, F. E. Close, A. Donnachie, J. Forshaw, L. Frankfurt, A. Hebecker, G. Ingelman, G. Kramer, P. Landshoff, G. Levin, M. Strikman, N. Nikolaev and W. J. Stirling have patiently tolerated my ignorance of the theoretical details of hadronic diffraction and QCD, and thereby influenced the presentation here of the experimental results. Without the close and productive collaboration of Andrew Mehta and Julian Phillips, the results and their interpretation presented here would not be.

References

[1] I. Abt et al. (H1 Collaboration), "The H1 Detector at HERA", DESY preprint DESY 93-103 (1993).

[2] B. Andrieu et al. (The H1 Calorimeter Group), Nucl. Inst. Meth. **A336** (1993) 460.

[3] B. Andrieu et al. (The H1 Calorimeter Group), Nucl. Inst. Meth. **A336** (1993) 499.

[4] H. I. Cronström et al. Nucl. Inst. Meth. **A340** (1994) 304.

[5] A. Mehta, "Measurement of the Diffractive Proton Structure Function and Calibration of the Forward Muon Detector at H1", PhD thesis (University of Manchester), 1994 (unpublished) and Rutherford Appleton Laboratory report RALT-037.

[6] T. Ahmed et al. (H1 Collaboration), Nucl. Phys. **B449** (1995) 3.

[7] M. Derrick et al. (ZEUS Collaboration) Phys. Lett. **B315** 481 (1993).

[8] W. Bartel, "$\sigma_{\gamma p}^{tot}$ and Diffractive Processes in Photoproduction and DIS.", in Proc. of the Europhysics Conference, Marseilles, France, July 1993, ed. J. Carr and M. Perrottet, p. 585.
J. B. Dainton, "Results from the H1 Experiment at HERA", in Proc. XVI International Symposium on Lepton Photon Interactions, Cornell, Ithaca, USA, August 1993, ed. P. Drell and D. Rubin, p. 87 and Rutherford Appleton Laboratory preprint RAL 94-12.
A. De Roeck, "Results from the H1 Experiment.", in Proc. of the Europhysics Conference, Marseilles, France, July 1993, ed. J. Carr and M. Perrottet, p. 791 and DESY preprint DESY 94-005 (1994).

[9] T. Ahmed et al. (H1 Collaboration), Nucl. Phys. **B429** (1994) 477.

[10] see for example
J. B. Dainton, "Physics at HERA", in Proc. Inst. of Phys. (IoP) Ann. Conf. on Particle Physics, Sheffield, UK, April 1990, IoP Short Meetings Series no. 26, ed. F. Combley, **ISBN 0-85498-526-3**, IoP Publishing, and references therein.
J. Ellis, in Proc. "Study of an *ep* Facility for Europe", ed. U. Amaldi, DESY 79-48 (1979).

[11] R. P. Feynman, "Photon Hadron Interactions", 1972, W. Benjamin Inc., **ISBN 0–805–32510–7**, p. 344.

[12] J. D. Bjorken, "Hard Diffraction and Deep–Inelastic Scattering", in Proc. of the Int. Workshop on Deep–Inelastic Scattering and Related Topics, Eilat, Israel, 1994, ed. Aharon Levy, World Scientific, **ISBN 981–02–2053–7**, p. 151, and earlier references therein.

[13] G. Ingelman and K. Janson–Prytz, "The Pomeron Structure Function and QCD at Small–x", in Proceedings of the Workshop "Physics at HERA", p. 233, October 1991, ed. W. Buchmüller and G. Ingelman.

[14] G. Ingelman and K. Prytz, Zeit. Phys. **C58** (1993) 285.

[15] T. Ahmed et al. (H1 Collaboration), Phys. Lett. **B348** (1995) 681.

[16] T. Ahmed et al. (H1 Collaboration), Nucl. Phys. **B439** (1995) 471.

[17] U. Bassler and G. Bernardi, "On the Kinematic Reconstruction of Deep Inelastic Scattering at HERA: the Sigma Method", DESY 94–231 (1994), submitted to Nucl. Instr. and Meth.

[18] G. Ingelman, "LEPTO 6.1", unpublished program manual, and in Proc. of the Workshop "Physics at HERA", 1366, ed. W. Buchmüller and G. Ingelman, Hamburg (1991).
H. Bengtsson, G. Ingelman and T. Sjöstrand, Nucl. Phys. **B301** (1988) 554.

[19] L. Lönnblad, Comput. Phys. Commun. **71** (1992) 15.

[20] H. Jung, Comput. Phys. Commun. **86** (1995) 147.

[21] T. Regge, Nuov. Cim. **14** (1959) 951, Nuov. Cim. **18** (1960) 947.

[22] G. Chew, S. Frautschi, S. Mandelstam, Phys. Rev. **126** (1962) 1202.

[23] P. Collins and E. Squires, "An Introduction to Regge Theory and High Energy Physics", Cambridge University Press, Cambridge (1977).

[24] A. Donnachie and P. Landshoff, Nucl. Phys. **B303** (1988) 634.

[25] L. N. Lipatov, Sov. Phys. JETP **63** (1986) 904.

[26] R. J. Eden, P. V. Landshoff, D. I. Olive, J. C. Polkinghorne, "The Analytic S-Matrix", Cambridge University Press, Cambridge (1966).

[27] É. A. Kuraev, L. N. Lipatov, and V. S. Fadin, Sov. Phys. JETP **45** (1977) 199.
Ya. Ya. Balitskiĭ and L. N. Lipatov, Sov. J. Nucl. Phys. **28** (1978) 822.

[28] M. Genovese, N. N. Nikolaev, B. G. Zakharov, "Diffractive DIS from the generalised BFKL pomeron. Predictions for HERA.", Institut für Kernphysik, KFA, Jülich preprint KFA–IKP(Th)–1994–37.

[29] T. Ahmed et al. (H1 Collaboration), Phys. Lett. **B354** (1995) 494.

[30] A. Mehta, "Comparison of Diffractive and non-Diffractive Deep–Inelastic Scattering", in Proc. of the International Workshop on Photon–Photon and Photon–Hadron Interactions "Photon95", Sheffield, UK, April 1995, ed. S. L. Cartwright and D. J. Miller, in litt.

[31] A. Caldwell, J. B. Dainton, W. J. Stirling et al., Report of the Working Group on Structure Functions, in Proc. of the Int. Workshop on Deep–Inelastic Scattering and Related Topics, Eilat, Israel, 1994, ed. Aharon Levy, World Scientific, **ISBN 981–02–2053–7**, p.315.

[32] B. Badelek, N. Brook, A. De Roeck, A. D. Martin et al., Report of the Working Group on Structure Functions, to appear in Proc. of the Phenomenology Workshop "Proton, Photon and Pomeron Structure", Durham, UK, September 1995, to be published in J. Phys. **G**.

[33] A. C. Benevenuti et al., Phys. Lett. **B223** (1989) 485; preprint CERN–EP/89-06.

[34] P. Amaudruz et al., Phys. Lett. **B295** (1992) 159; preprint CERN–EP/92-124.

[35] Yu. L. Dokshitzer, JETP **46** (1977) 641.
V. N. Gribov and L. N. Lipatov, Sov. Journ. Nucl. Phys. **15** (1972) 78.
G. Altarelli and G. Parisi, Nucl. Phys. **B126** 1977 298.

[36] C. Pascaud, F. Zomer, LAL preprint LAL/94-42.

[37] J. P. Phillips, "Rapidity Gap Events at HERA and the Structure of the Pomeron", in Proc. of the International Workshop on Deep–Inelastic Scattering and Related Topics, Paris, France, April 1995, ed. J-F. Laporte and Y. Sirois, in litt.

[38] Ch. Berger et al. (PLUTO Collaboration), Zeit. Phys. **C26** 353 (1984).

[39] H. Abramowicz, K. Charchula, A. Levy, Phys. Lett. **B269** (1991) 450.

[40] M. Glück, E. Reya and A. Vogt, Phys. Rev. **D46** (1992) 1973.

[41] E. Witten, Nucl. Phys. **B120** (1977) 189.

[42] W. Buchmüller, A. Hebecker, "A Parton Model for Diffractive Processes in Deep–Inelastic Scattering", DESY preprint DESY 95–077 (1995).

[43] H. Kowalski, talk presented in the Diffractive Working group at the Int. Workshop on Deep–Inelastic Scattering and Related Topics, Eilat, Israel, February 1994.